

pubs.acs.org/JPCB Article

Solution-based Supramolecular Hierarchical Assembly of Frenkel Excitonic Nanotubes Driven by Gold Nanoparticle Formation and Temperature

Seda Kelestemur, Piyali Maity, Nikunjkumar R. Visaveliya, Damien Halpern, Sadiyah Parveen, Firdaus Khatoon, Ali Khalil, Matthew Greenberg, Qingrui Jiang, Kara Ng, and Dorthe M. Eisele*



Cite This: J. Phys. Chem. B 2024, 128, 329-339



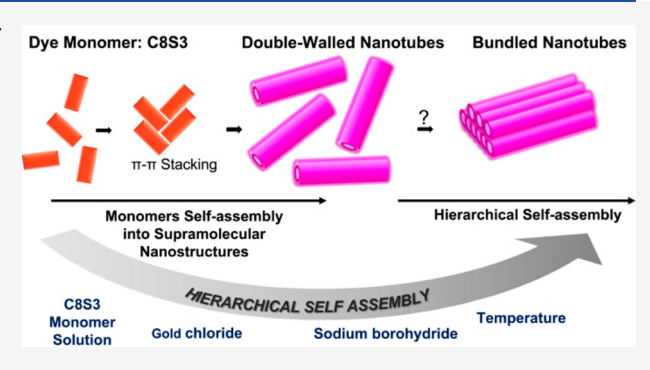
ACCESS

III Metrics & More

Article Recommendations

Supporting Information

ABSTRACT: Translating nature's successful design principle of solution-based supramolecular self-assembling to broad applications—ranging from renewable energy and information technology to nanomedicine—requires a fundamental understanding of supramolecular hierarchical assembly. Though the forces behind self-assembly (e.g., hydrophobicity) are known, the specific mechanism by which monomers form the hierarchical assembly still remains an open question. A crucial step toward formulating a complete mechanism is understanding not only how the monomer's specific molecular structure but also how manifold environmental conditions impact the self-assembling process. Here, we elucidate the complex correlation between the environmental self-assembling conditions and



the resulting structural properties by utilizing a well-characterized model system: well-defined supramolecular Frenkel excitonic nanotubes (NTs), self-assembled from cyanine dye molecules in aqueous solution, which further self-assemble into bundled nanotubes (b-NTs). The NTs and b-NTs inhabit distinct spectroscopic signatures, which allows the use of steady-state absorption spectroscopy to monitor the transition from NTs to b-NTs directly. Specifically, we investigate the impact of temperature (ranging from 23 °C, 55 °C, 70 °C, 85 °C, up to 100 °C) during in situ formation of gold nanoparticles to determine their role in the formation of b-NTs. The considered time regime for the self-assembling process ranges from 1 min to 8 days. With our work, we contribute to a basic understanding of how environmental conditions impact solution-based hierarchical supramolecular self-assembly in both the thermodynamic and the kinetic regime.

1. INTRODUCTION

Hierarchical assembly—resulting in materials with order at multiple length scales—is nature's most successful design principle to form functional systems. 1-4 Examples for hierarchical self-assembly in biological systems range from DNA, keratin, collagen, cell membranes, tiny photosynthetic bacteria, dendron virus, algae, and silk fibers to bones, and in nature range from nacre, eggshells, carrots, or navy beans to even large trees. 5-17 One of the most well-known examples of supramolecular hierarchical self-assembly is the formation of collagen, the primary component of connective tissue in mammals: three polypeptide strands first twist into a righthanded triple helix, which subsequently self-assemble into socalled microfibrils, with these microfibrils then further assembling into larger collagen fibers. 18 In nature, each level of hierarchy—from molecule, to supramolecular building block, to close-packed building blocks-plays an important role in the system's intimate structure-function relationship. 19-25 Gaining a detailed understanding of the fundamental self-assembly process is the pivotal next step for any future applications of hierarchical assembly.

While the main forces that drive the supramolecular self-assembling process are known—for example, hydrophobicity for amphiphilic monomers^{26–28}—studying the intimate correlation between the specific self-assembling conditions and the resulting structural properties is known to be experimentally challenging and therefore remains an open question.

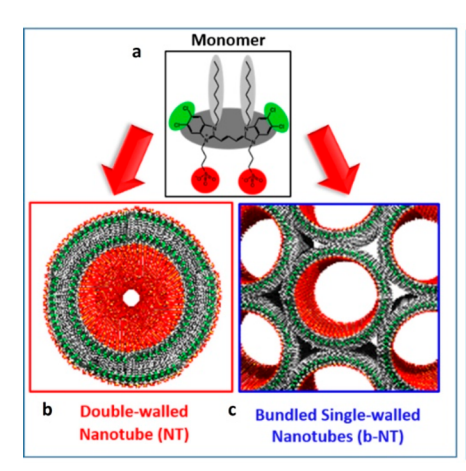
For solution-based supramolecular self-assembly processes, not only the makeup of the specific molecule—such as chemical structure and its concentration—but also the overall environmental conditions of the solution are critical factors. ^{29–33} For example, the solubility of the solute, solvent polarity, solute—solvent interaction, or solvent concentration

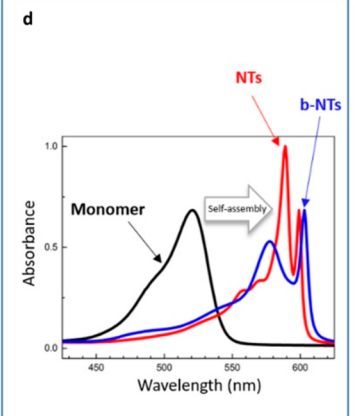
Received: August 22, 2023
Revised: November 10, 2023
Accepted: November 10, 2023

Published: December 29, 2023









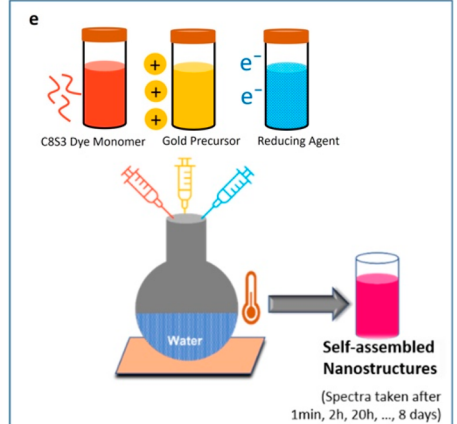


Figure 1. Supramolecular Frenkel excitonic nanotubes and experimental setup. (a) C8S3 dye monomer. (b) Schematic of double-walled nanotube (NT). (c) Schematic of bundled nanotube (b-NT) with surrounding outer envelope layer (not shown). (d) Absorption spectra of C8S3 dye monomer, NTs and b-NTs in solution. (e) Cartoon depicting experimental design to study formation of self-assembled nanostructures. Schematics of NT and b-NT in panels b and c are adapted from ref 69.

can impact the self-assembly process and resulting nanostructures. 34–43 Depending on relatively weak, noncovalent interactions, most supramolecular assemblies are under thermodynamic control, and research on, for example, supramolecular polymers has focused predominantly on equilibrium conditions. 44–52 However, there is an increasing interest in self-assembly processes that are governed by kinetics, where the outcome of the assembly process is dictated by the assembly pathway rather than the free energy of the final assembled state. 44,53–55

Here, considering both thermodynamic and kinetic regime, we investigate the complex correlation between the environmental self-assembling conditions and the resulting structural properties by utilizing a well-characterized, well-defined artificial supramolecular model system: synthetic molecular chromophores of the amphiphilic cyanine dye 3,3'-bis(2sulfopropyl)-5,5',6,6'-tetrachloro-1,1'-dioctylbenzimidacarbocyanine (dye monomer commonly abbreviated as C8S3, Figure 1a) self-assemble in aqueous solution into highly uniform bilayered (double-walled) supramolecular nanotubes (NTs) with an inner cylinder and an outer cylinder as depicted in Figure 1b. 34,56-68 The NT's formation is thought to be mainly driven by a superposition of the dispersion force of the pi-pi stacking of the dye monomer's aromatic rings and the hydrophobic forces governed by the monomer's amphiphilic side chains. These NTs are known to form well-characterized hierarchical structures, that is, bundles of single-walled nanotubes (b-NTs, Figure 1c).⁶⁹ Similar to the structure of the double-walled NTs, it is reasonable to expect that the b-NTs are surrounded by an outer envelope layer of selfassembled dye molecules that expose their hydrophilic heads to the aqueous solution.⁶⁹

Overall, even though this NT system has been intensively studied, ^{69,70} the details of its self-assembling process are not understood yet. For example, experimental studies requiring b-NTs still rely on a rather uncertain sample preparation such as incubating NTs at room temperature in the dark, where the formation of b-NTs can take from days up to several months. ⁶⁹ The mechanism as well as specific driving forces behind the hierarchical self-assembly process—leading to the formation of b-NTs—is still unknown.

In this study, we take advantage of the circumstance that the two distinct, well-defined supramolecular morphologies—that is, double-walled NTs (Figure 1b) and bundles of single-walled NTs (Figure 1c)—show two distinct, well-defined spectroscopic signatures (Figure 1d) as described elsewhere. 34,56-77 In short, upon initiation of the self-assembly process, the broad absorption spectrum of the C8S3 monomers undergoes a large shift toward lower energy (red-shift) accompanied by a substantial narrowing of the absorption bands (Figure 1d) both characteristic features of so-called J-aggregates 54,71,72 or Scheibe aggregates.⁷³ The close-packing arrangement of the C8S3 monomers within the NTs causes excitation transfer interactions between the monomers' transition dipole moments that results into new electronic states, delocalized Frenkel excitons. 74-79 As these delocalized excited states intimately depend on the details of the supramolecular assemblies' molecular packing, the optical properties of the NTs are highly sensitive to the details of the supramolecular structure. 80-82 Figure 1d (red solid line) shows the welldefined spectroscopic signature of double-walled NTs in aqueous solution: the narrow exciton band at 599 nm and broad exciton band at 589 nm are originated by parallel polarized exciton transitions of the NT's inner-wall and outerwall cylinder, respectively. The shoulder around 580 nm and features at higher energies result from perpendicular polarized exciton transitions from both the NT's inner-wall and outerwall cylinders.^{34,83} Figure 1d (blue solid line) shows the spectroscopic signature of bundled NTs in aqueous solution: the narrow exciton band at 603 nm and a broad absorption feature around 580 nm mainly originated by parallel polarized and perpendicular polarized exciton transitions of the bundled inner-wall cylinders, respectively.⁶⁹ Previous studies suggested that the surrounding outer envelope layer of b-NTs contributes to the absorption spectrum not with narrow exciton bands but rather with a spectrally broad distribution of bands, consistent with an inhomogeneous supramolecular structure.⁶⁹ As the three morphologies in solution—dye monomers, NTs, and b-NTs-can be clearly distinguished by their well-defined spectroscopic signatures, convenient steady state absorption spectroscopy can be utilized as an elegant tool to correlate the specific self-assembly conditions and the resulting structural properties during the self-assembling process.

By employing absorption spectroscopy, this work focuses on studying the impact of temperature (ranging from 23 °C, 55 °C, 70 °C, 85 °C, up to 100 °C) during in situ formation of gold nanoparticles (AuNPs) on the hierarchical assembly formation of b-NTs from C8S3 monomers in aqueous solution, considering a time regime ranging from 1 min up to 8 days (Figure 1e). With this work, via a temperature-dependent reaction in the presence of AuNPs formation, we can control the hierarchical self-assembly process of NTs resulting in b-NTs.

2. METHODS

2.1. Chemicals. The amphiphilic cyanine dye 3,3′-bis(2-sulfopropyl)-5,5′,6,6′-tetrachloro-1,1′-dioctylbenzimidacarbocyanine (commonly abbreviated as C8S3) is available as a sodium salt (Na⁺) from FEW Chemicals (Dye S 0440, molecular weight = 902.8 g mol⁻¹; FEW Chemicals GmbH, Germany) and was used as received. Both the gold(III) chloride (99%, molecular weight = 303.33 g mol⁻¹) and the sodium borohydride (\geq 98.0%, molecular weight = 37.83 g mol⁻¹), as well as pure methanol, are available from Millipore-Sigma. Ultrapure H₂O (>18.2 M Ω cm, Millipore) was used for the synthesis of the supramolecular self-assembled nanostructures. All the chemicals were used as received without any further purification.

2.2. Preparation of Stock Solutions. *C8S3 Dye Stock Solution (C8S3 Monomer Solution).* A 3.00 mM C8S3 monomer solution was prepared by dissolving 57.6 mg of C8S3 (MW= 902.8 g/mol) in 20 mL of pure methanol under continuous stirring. The color of the obtained C8S3 monomer solution was dark orange-red.

Gold Chloride Stock Solution (Metal Precursor Solution). A 0.5 mM metal precursor solution was prepared by dissolving 1.5 mg of gold(III) chloride (AuCl₃) in 10 mL of ultrapure H₂O under continuous stirring.

Sodium Borohydride Solution (Reducing Agent Solution). A 0.01 M reducing agent solution was prepared by dissolving 3.78 mg of sodium borohydride in 10 mL of ultrapure $\rm H_2O$) under continuous stirring.

2.3. Preparation of Bundled Nanotubes (b-NTs). *b-NT Synthesis Step 1.* In Step 1, a round-bottom flask (RBF) with 2.5 mL of ultrapure H_2O was placed in the oil bath and heated up to 70 °C by using a Fisher Scientific hot plate stirrer with a digital temperature probe. The temperature of the aqueous solution was measured by using an Etekcity infrared thermometer. Then, to the ultrapure H_2O at 70 °C, 250 μ L of the C8S3 monomer solution was added slowly (drop by drop, over a time of about 2 min) by using a micropipette. This aqueous C8S3 solution was stirred for 2 min. Next, 2.5 mL of the metal precursor (0.5 mM gold chloride stock solution) was added and stirred for an additional 2 min. Further, 0.3 mL of the reducing agent (0.01 M sodium borohydride solution) was added and kept stirring for 25 min.

b-NT Synthesis Step 2. In Step 2, an additional 200 μ L of C8S3 monomer solution was added into the solution, as described in Step 1, and stirred for 20.

Temperature Dependence. The procedure (Step 1 and Step 2) was performed for every single sample prepared at different temperatures: at 23 °C (room temperature), 55 °C, 70 °C, 85 °C, and 100 °C. A summary table including reaction conditions and results is given in Table S1 in Supporting Information.

Control Experiment. As a control experiment, we studied the effect of increased temperature at 70 °C without the formation of AuNPs. For the control experiment, all of the experimental conditions were performed as described above (Step 1 and Step 2) at 70 °C but without adding metal precursor gold chloride stock solution and reducing agent sodium borohydride solution. For details, please see Table S2 in Supporting Information.

2.4. Characterization Techniques. Optical Characterization (Room Temperature UV–visible Spectroscopy). We performed UV–vis spectroscopic measurements to monitor self-assembly of cyanine dye monomers to the b-NTs. For this experiment, a single-beam UV–visible spectrometer purchased from Agilent Technologies (Model Number: Cary 8454) with a tungsten (G1315A, 8453) and a deuterium lamp (8453 UV–vis) was used. The UV–visible spectra of samples (200 μ L) were obtained using a quartz cell of path length 0.1 cm at room temperature in a time-dependent manner. Similarly, ultrapure water was used as a blank.

Structural Characterization (Transmission Electron Microscopy, TEM). Transmission Electron Microscopy (TEM) was used to visualize the morphology of b-NTs. The samples were prepared on an ultrathin carbon grid, and high-resolution transmission electron micrographs were captured using an FEI Titan Themis 200 kV instrument. 2.5 μ L of b-NTs were deposited on glow-discharged lacey carbon grids with ultrathin carbon film (Ted Pella; 01895-F) and imaged at TEM FEI Titan Themis operating at 200 kV.

3. RESULTS AND DISCUSSION

In general, in solution-based self-assembly processes, higher temperature can lead to higher molecule mobility—altering the dispersion forces of the pi-pi stacking—and can therefore lead to structural phase transitions by overcoming the kinetic limitations. ^{84–91} We investigate the impact of temperature on the self-assembling process by adding C8S3 monomers to aqueous solution preheated at different temperatures ranging from room temperature (23 °C), 55 °C, 70 °C, 85 °C, up to 100 °C, respectively. Furthermore, for cyanine dye, it was previously found that environmental conditions such as the type of counterion accompanying the chromophores of dye molecules may influence the morphology of the resulting supramolecular assemblies⁹² Here, the C8S3 dye monomers (used as received) are accompanied by Na+ as counterions as described in the Method Section. To probe the impact of counterions on the formation of hierarchically assembled b-NTs, we added Au⁺ ions (AuCl₃) to the aqueous solution after adding the dye monomer. To prevent oxidation of the C8S3 chromophore through reduction of Au⁺ ions, we added sodium borohydride (reducing agent), subsequently resulting in the formation of Au nanoparticles (NPs). 37,56,93 As the redox reaction of AuCl₃ and sodium borohydride does not require heat, it is described as a so-called "cold" redox reaction. To monitor the participation of C8S3 dye monomers in the hierarchical self-assembling process in the presence of AuNPs, we added additional C8S3 dye monomer (see the Methods Section, Part 2.3, Step 2) to the ongoing reaction.

We hypothesize that both increased temperature and in situ formation of AuNPs may drive the hierarchical self-assembly process—that is, formation of b-NTs—via impacting the $\pi-\pi$ stacking process due to increased molecule mobility and capillary forces. Furthermore, we hypothesize that upon addition of Au⁺ ions, the increase of the solvent's dielectric

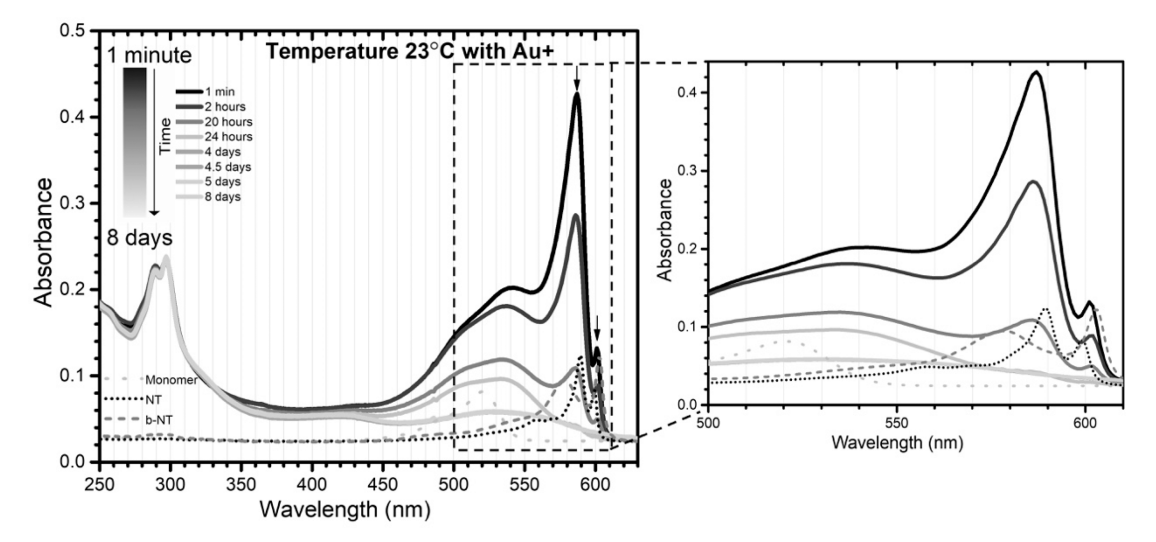


Figure 2. Supramolecular hierarchical assembly in the presence of Au⁺ and reducing agent at 23 °C. Absorption spectra of supramolecular assembly of cyanine dyes taken after 1 min (black line) of sample preparation as well as 2 h, 20 h, 24 h, 4 days, 4.5 days, 5 days, and 8 days (gray shade lines). For comparison, reference spectra of monomer (light gray, dotted line), NTs (black, short dotted line), and b-NTs (gray, short dashed line) solution from Figure 1d are shown.

constant and decrease of repulsive forces between the NTs may result in direct formation of b-NTs. 97,98

We support our two hypotheses as follows. In general, the formation of NTs from C8S3 dye monomers occurs immediately upon the addition of the dye monomers to the aqueous solution. In this study, the Au salt was added to the aqueous solution 2 minutes after the C8S3 dye monomer addition, allowing Au⁺ ions to interact with the occurred NTs during the ongoing NT formation. Within the time window before adding the reducing agent, in addition to their role as counterions, the gold ions may also interact with the NT's negatively charged hydrophilic SO3-. According to our hypothesis, the negatively charged AuNPs may interact with the negatively charged b-NTs, potentially stabilizing the b-NTs. It is possible, even though both species are negatively charged, that b-NTs prefer to be in close proximity to AuNPs due to differences in their charge densities. 99 Also, the negatively charged AuNPs may increase the repulsive forces between the negatively charged NTs. 100 Furthermore, in addition to prevention of potential oxidation of the C8S3 chromophores, the added reducing agent sodium borohydride may have a stabilizing effect on the formed b-NTs.

As a first step, we added Au salt and reducing agent, respectively, to an aqueous solution at room temperature (23 \pm 1 °C) followed by addition of C8S3 monomers as described in the Methods Section. The absorption spectra were taken 1 min after sample preparation (black line) as well as after incubation for 2 h, 20 h, 24 h, 4 days, 4.5 days, 5 days, and 8 days (gray shade lines) are depicted in Figure 2. In reference to the broad C8S3 monomer spectrum shown in Figure 1d, the absorption spectrum taken 1 min directly after sample preparation reveals a strong red-shift with complex spectral features, including a narrow band at 601 nm and an excitonic band at 587 nm. Both features, the red-shift and line narrowing, indicate the formation of a molecular assembly via pi-pi-stacking with Frenkel excitonic (J-aggregate) character. However, overall, the absorption spectrum resembles the spectroscopic characteristic for neither double-walled NPs nor b-NTs. Utilizing sophisticated cryogenic electron microscopy (cryo EM), previous studies correlated supramolecular assemblies formed from amphiphilic cyanine dye derivatives with their morphology suggested that absorption spectra such as observed in Figure 2 can be correlated to rather ill-defined so-called ribbon-like aggregate structures. ^{68,101}

Another interesting feature in Figure 2 is that it is located in the UV region. In addition to the exciton bands (J-bands) in the visible region, UV absorbance bands appear around 300 nm, which indicates formation of C8S3 dimers due to oxidation of the C8S3 chromophores. 102 Previous spectroelectrochemistry studies of NTs revealed that upon electrochemical oxidation, the decrease of the exciton bands in the visible region is also simultaneously accompanied by an increase of two additional UV absorbance bands at 210 and $300 \text{ nm.}^{102-104}$ However, even though the exciton bands in the visible region substantially decrease within 24 h after sample preparation, the absorbance bands around 300 nm (oxidation) do not significantly increase. This observation suggests that the ongoing loss in exciton band absorption over the time window of 8 days may not be caused by oxidation of the C8S3 chromophores but potentially by partial precipitation, which might be caused by the interaction of the AuNPs with the supramolecular assembly of ill-defined morphology. This partial participation can be explained by the aggregation behavior of nanoparticles. Nanoparticles can easily aggregate through a thermodynamically driven process to reduce their high surface energies. 105 The Frenkel excitonic assemblies, which are in close interaction with the AuNPs, can be triggered by AuNPs and precipitated together during the incubation. The weak capillary forces in the aqueous solution can cause precipitation in the presence of AuNP. 42,105-108 This precipitation can also be explained with the addition of additional monomer in the middle of the reaction after formation of AuNPs in aqueous solution. It is possible that the additional monomers adsorb on the surface area of nanoparticles very easily, reducing the stability of the suspended AuNPs in aqueous solution and causing partial precipitation together with the Frenkel excitonic assemblies within 24 h. 108 In the following, we study the impact of temperature on the hierarchical self-assembling process in the presence of Au⁺ ions and reducing agent.

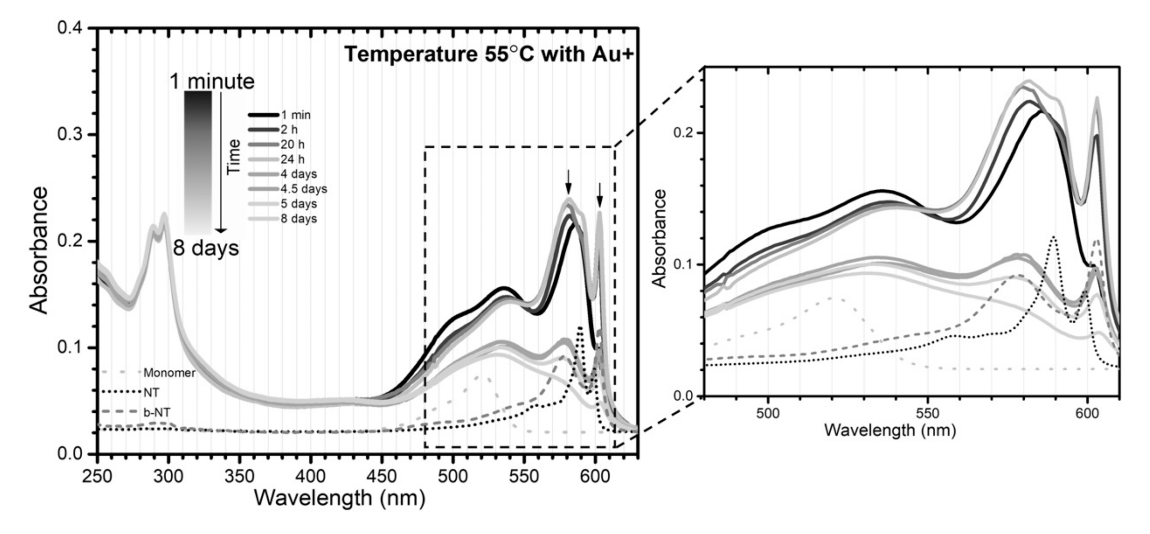


Figure 3. Supramolecular hierarchical assembly in the presence of Au⁺ and reducing agent at 55 °C. Absorption spectra of supramolecular assembly of cyanine dye taken after 1 min (black line) of sample preparation as well as 2 h, 20 h, 24 h, 4 days, 4.5 days, 5 days, and 8 days (gray shade lines). The spectra reveal the formation of the bundled nanotubes with a loss in excitonic character over time. For comparison, reference spectra of monomer (light gray, dot line), NTs (black, short dot line), and b-NTs (gray, short dash line) solution from Figure 1d are included.

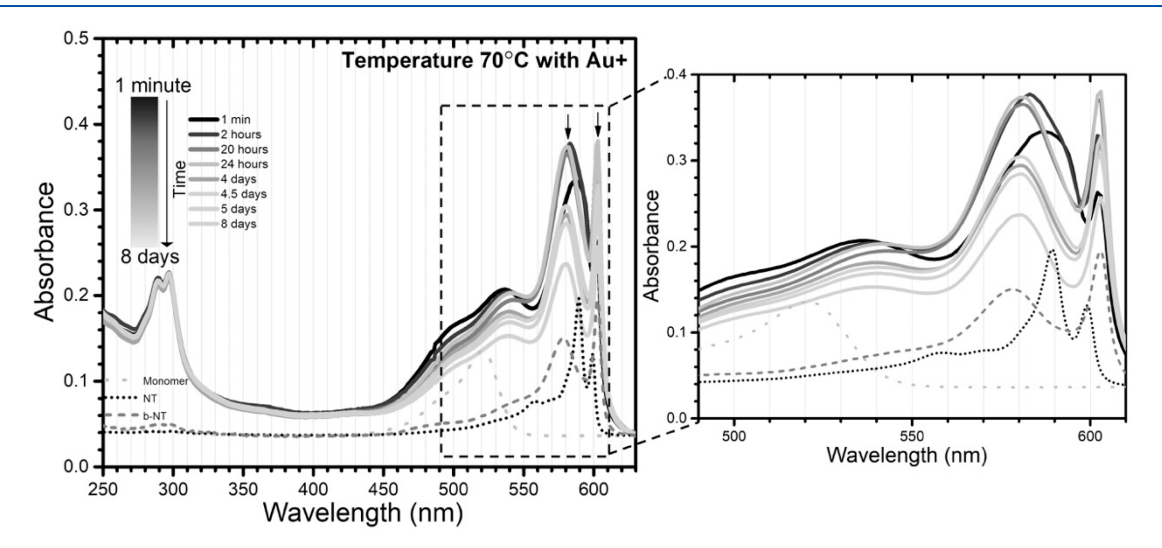


Figure 4. Supramolecular hierarchical assembly in the presence of Au⁺ and reducing agent at 70 °C. Absorption spectra of supramolecular assembly of cyanine dye taken after 1 min (black line) of sample preparation as well as 2 h, 20 h, 24 h, 4 days, 4.5 days, 5 days, and 8 days (gray shade lines). The spectra reveal the formation of the bundled nanotubes, which retained their excitonic character during incubation. For comparison, reference spectra of monomer (light gray, dot line), NTs (black, short dot line), and b-NTs (gray, short dash line) solution from Figure 1d are displayed.

Figure 3 depicts the absorption spectra taken 1 min after sample preparation (black line) as well as after incubation for 2 h, 20 h, 24 h, 4 days, 4.5 days, 5 days, and 8 days (gray shade lines), respectively, at 55 ± 1 °C. The absorption spectrum taken 1 min directly after sample preparation reveals a strong red-shift including a narrow band at 604 nm—significantly visible after 2 h incubation—and a broad band around 580 nm. These red-shifted absorption spectra indicate formation of b-NTs after 2 h of incubation in reference to Figure 1d. As the incubation period increased, b-NTs lost their excitonic character due to the partial precipitation of the Frenkel excitonic assemblies in the presence of AuNP. $^{42,105-108}$ In the following, we study the impact of the 70 °C temperature on the hierarchical self-assembling process in the presence of Au+ions and reducing agent.

Figure 4 shows the absorption spectra of NTs taken 1 min after sample preparation (black line) as well as after incubation for 2 h, 20 h, 24 h, 4 days, 4.5 days, 5 days, and 8 days (gray

shade lines) at a temperature of $70\pm1\,^{\circ}$ C. A narrow excitonic band at 604 nm attributed to the inner cylinder and the broad exciton band at 580 nm belonging to the outer cylinder of b-NTs are observed, as seen in Figure 4. In a higher energy region, a broad absorbance band at 535 nm is attributed to the absorbance of AuNPs. Although the excitonic bands in the visible region decreased with the increase incubation time due to the partial precipitation in the presence of AuNPs, $^{42,105-111}$ the bundle structure of the NTs remained intact. This result supports our hypothesis; the high temperature increased the molecular mobility and promoted the bundling process of the cyanine dye monomers through the contribution of the gold ions.

Monomer and dimer ion pairs between dyes and metal ions are considered to serve as reactants for the J-aggregated hierarchical arrangement. It is reasonable to assume that metal ions produce ion pairs with the dye, where the inherent counterion (Na^+) is replaced by the metal ion at an

appropriate salt concentration. ⁹² In the following, we study the morphology of prepared b-NTs and also the impact of higher temperature on the hierarchical self-assembling process in the presence of Au⁺ ions and a reducing agent.

Figure 5a, 5b, and 5c displays transmission electron micrographs (TEM) at different magnification scales of the

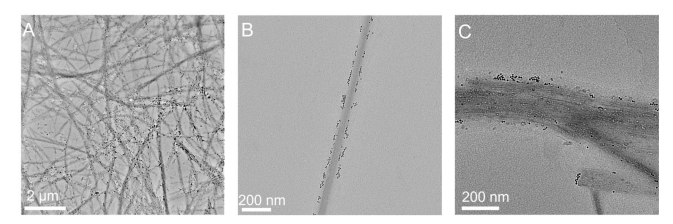


Figure 5. TEM images of supramolecular hierarchical assembly in the presence of $\mathrm{Au^+}$ at 70 °C. Bundled nanotubes (b-NTs) assembled from the cyanine dye monomers (driven by the formation of AuNPs at 70 °C). (A–C) Transmission electron micrographs at different magnification. The black spherical dots represent the AuNPs.

hierarchical supramolecular self-assemblies and spherical AuNPs prepared at 70 \pm 1 °C, demonstrating the b-NT morphology with an average diameter of 45 \pm 1 nm. The tiny gold nanoparticles (AuNPs) with an average diameter of 3.0 \pm 0.1 nm on the surfaces of nanotubes are observed. We can explain this close interaction of the gold nanoparticles with NTs based on their charge-density differences. 99

Figure 6a and 6b show the absorption spectra taken 1 min after sample preparation (black line) as well as after incubation for 3, 3.5, 4, and 7 days (gray shade lines) at 85 ± 1 °C and 100 ± 1 °C. The absorption spectra taken 1 min directly after sample preparation at 85 ± 1 °C and 100 ± 1 °C demonstrate only the formation of AuNPs observed at 535 nm. Spectra taken after 3 days reveal a strong red-shift with a narrow band at the visible region around 580 nm. Red-shift, along with line narrowing, indicate the formation of a molecular assembly via pi–pi stacking J-aggregate character. However, overall, the absorption spectra resembles the spectroscopic characteristic for neither NTs nor b-NTs. They can be correlated to quasi-one-dimensional-like aggregate structures. 67

The absorbance of the excitonic band at 580 nm slowly increased during incubation, while the absorbances of bands around 300 nm decreased. This shows that the cyanine monomers could not self-assemble into J-aggregates during the reaction due to the very high temperatures. The formation of J-aggregates was observed after incubation of the suspension at room temperature for 3 to 7 days. One of our previous studies also showed the formation of quasi-one-dimensional-like aggregates after silica-scaffolded NTs were exposed to a heat-stress. 112,113

Figure 7 depicts the absorption spectrum taken 1 min after sample preparation (black line) and after incubation for 2 h, 24 h, 2 days, and 4 days (gray shade lines) at (70 ± 1) °C as a control experiment as described in the Methods Section. In reference to the broad C8S3 monomer spectrum shown in Figure 1d, the absorption spectra reveal a strong red-shift with spectral features including a narrow excitonic band at 604 nm—significant after 24 h incubation—and a broad excitonic band at around 580 nm attributed to b-NTs. Thus, the result suggests that the temperature of 70 \pm 1 °C is directly impacting the hierarchical self-assembly of b-NTs. However, the b-NTs lost their bundled structure after a 4-day incubation. This finding proves our hypothesis about the stability effect of AuNPs on the structure of the b-NTs due to differences between their charge densities and increased repulsive forces in aqueous solution. 99,100

4. CONCLUSIONS

We have demonstrated a systematic study elucidating hierarchical supramolecular self-assembly at different temperatures (23 °C, 55 °C, 70 °C, 85 °C, up to 100 °C) and in the presence of counterions and a reducing agent. We found that both temperature and counterions (gold ions) play a role in driving the direct formation of hierarchical supramolecular assembly of b-NTs by pi-pi-interacted molecular self-assembly, while the AuNPs have a significant impact on stability of b-NTs. Specifically, we found that direct formation of b-NTs occurs at 55 and 70 °C in the presence of AuNPs. However, the b-NTs are only stable when the reaction occurs at 70 °C. Furthermore, we found that the increased

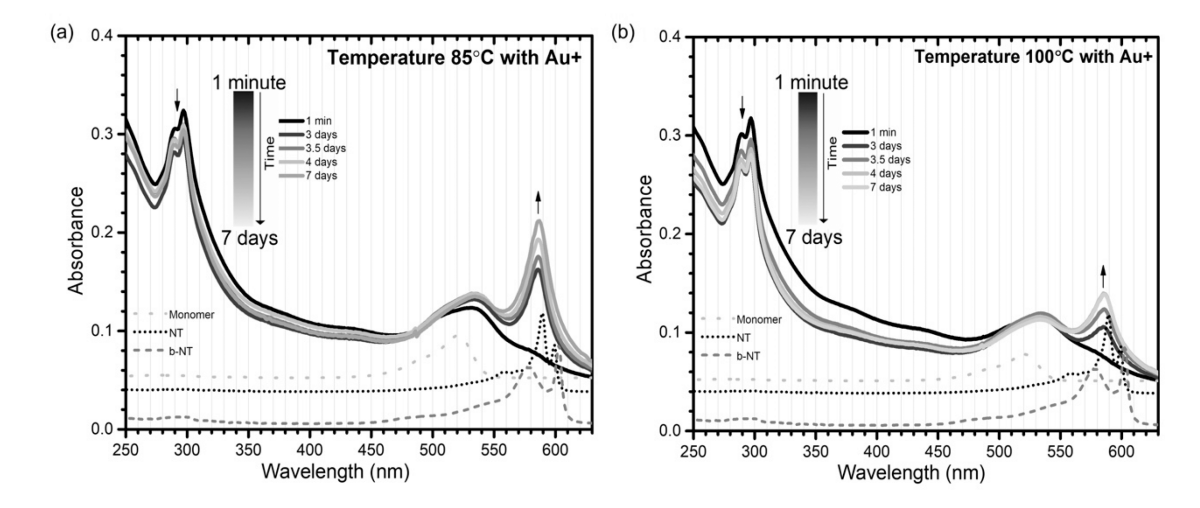


Figure 6. Supramolecular hierarchical assembly in the presence of Au⁺ and reducing agent at 85 and 100 °C. Absorption spectra of supramolecular assembly of cyanine dye taken after 1 min (black line) of sample preparation as well as 3 days, 3.5 days, 4 days, and 7 days (gray shade lines). The spectra reveal the formation of the C8S3 assembly with J-aggregate character after incubation for 3 to 7 days. For comparison, reference spectra of monomer (light gray, dotted line), NTs (black, short dotted line), and b-NTs (gray, short dash line) solution from Figure 1d are shown.

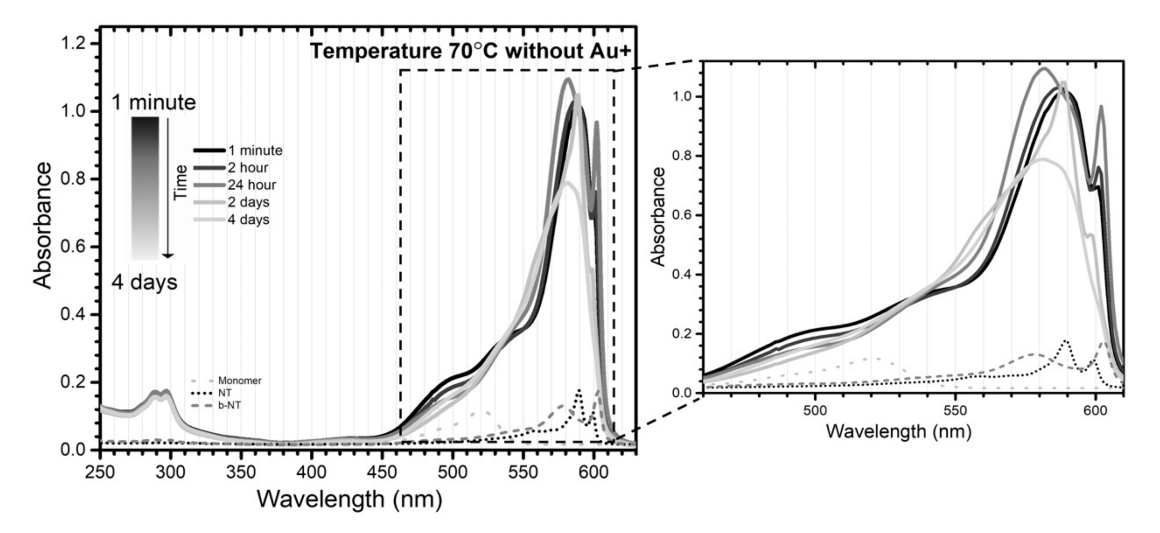


Figure 7. Supramolecular hierarchical assembly without Au⁺ at 70 °C. Absorption spectra of supramolecular assembly of cyanine dye taken after 1 min (black line) of sample preparation as well as 2 h, 20 h, 24 h, 2 days, and 4 days (gray shade lines) to monitor spectral changes. For comparison, reference spectra of monomer (light gray, dotted line), NTs (black, short dotted line), and b-NTs (gray, short dash line) solution from Figure 1d are shown.

temperature of 70 $^{\circ}$ C directly impacts the b-NTs formation, while the stability of b-NTs is supported in the presence of AuNPs. Within this study, we obtained stable b-NTs with a diameter of 45 \pm 1 nm in only 45 min, which eliminates the need for long incubation periods (from days up to several months) for the hierarchical self-assembly of NTs to b-NTs. Overall, with our work, we contribute to a fundamental understanding of hierarchical self-assembly through controlling the process thermodynamically and kinetically.

ASSOCIATED CONTENT

Supporting Information

The Supporting Information is available free of charge at https://pubs.acs.org/doi/10.1021/acs.jpcb.3c05681.

Summary tables including reaction conditions, control experiment conditions, and summary of the results (PDF

AUTHOR INFORMATION

Corresponding Author

Dorthe M. Eisele — Department of Chemistry and Biochemistry, The City College of New York at The City University of New York, New York City, New York 10031, United States; ○ orcid.org/0000-0002-0986-1953; Email: eisele@eiselegroup.com

Authors

Seda Kelestemur – Department of Chemistry and Biochemistry, The City College of New York at The City University of New York, New York City, New York 10031, United States; Biotechnology Department, Institute of Health Sciences, University of Health Sciences, Istanbul 34668, Turkey

Piyali Maity – Department of Chemistry and Biochemistry, The City College of New York at The City University of New York, New York City, New York 10031, United States

Nikunjkumar R. Visaveliya — Department of Chemistry and Biochemistry, The City College of New York at The City University of New York, New York City, New York 10031, United States; orcid.org/0000-0001-8704-2120

Damien Halpern – Department of Chemistry and Biochemistry, The City College of New York at The City University of New York, New York City, New York 10031, United States

Sadiyah Parveen — Department of Chemistry and Biochemistry, The City College of New York at The City University of New York, New York City, New York 10031, United States

Firdaus Khatoon – Department of Chemistry and Biochemistry, The City College of New York at The City University of New York, New York City, New York 10031, United States

Ali Khalil – Department of Chemistry and Biochemistry, The City College of New York at The City University of New York, New York City, New York 10031, United States

Matthew Greenberg — Department of Chemistry and Biochemistry, The City College of New York at The City University of New York, New York City, New York 10031, United States

Qingrui Jiang – Department of Chemistry and Biochemistry, The City College of New York at The City University of New York, New York City, New York 10031, United States

Kara Ng — Department of Chemistry and Biochemistry, The City College of New York at The City University of New York, New York City, New York 10031, United States; PhD Program in Chemistry, Graduate Center of The City University of New York, New York City, New York 10016, United States

Complete contact information is available at: https://pubs.acs.org/10.1021/acs.jpcb.3c05681

Notes

The authors declare no competing financial interest.

ACKNOWLEDGMENTS

This material is based upon work partially supported by the National Science Foundation Faculty Early Career Development Program (NSF-CAREER 1752475) and the U.S. Department of Energy, Office of Science, Office of Basic Energy Sciences (DOE DE-SC0018142). Equipment support

is partially provided by the National Science Foundation Major Research Instrumentation Program (NSF-MRI 1531859). Support partially provided by the National Science Foundation NSF-CREST Center for Interface Design and Engineered Assembly of Low Dimensional Systems (IDEALS), NSF grant number NSF-CREST HRD-1547830. This work was performed at the Center for Discovery and Innovation of The City College of New York and the Advanced Science Research Center Imaging Facility of The City University of New York. The authors thank the PSC-CUNY Research Award Program for support.

REFERENCES

- (1) Katiyar, N. K.; Goel, G.; Hawi, S.; Goel, S. Nature-inspired materials: Emerging trends and prospects. *NPG Asia Mater.* **2021**, *13*, 1–16
- (2) Elemans, J. A.; Rowan, A. E.; Nolte, R. J. Mastering molecular matter. Supramolecular architectures by hierarchical self-assembly. *J. Mater. Chem.* **2003**, *13*, 2661–2670.
- (3) Huo, G.-F.; Shi, X.; Tu, Q.; Hu, Y.-X.; Wu, G.-Y.; Yin, G.-Q.; Li, X.; Xu, L.; Ding, H.-M.; Yang, H.-B. Radical-induced hierarchical self-assembly involving supramolecular coordination complexes in both solution and solid states. *J. Am. Chem. Soc.* **2019**, *141*, 16014–16023.
- (4) Wang, L.-M.; Yue, J.-Y.; Zheng, Q.-Y.; Wang, D. Temperature-Directed Hierarchical Surface Supramolecular Assembly. *J. Phys. Chem. C* **2019**, *123*, 13775–13781.
- (5) Lin, T.; Yan, J.; Ong, L. L.; Robaszewski, J.; Lu, H. D.; Mi, Y.; Yin, P.; Wei, B. Hierarchical assembly of DNA nanostructures based on four-way toehold-mediated strand displacement. *Nano Lett.* **2018**, 18, 4791–4795.
- (6) Hayes, O. G.; Partridge, B. E.; Mirkin, C. A. Encoding hierarchical assembly pathways of proteins with DNA. *Proc. Natl. Acad. Sci. U.S.A.* **2021**, *118*, No. e2106808118.
- (7) Cera, L.; Gonzalez, G. M.; Liu, Q.; Choi, S.; Chantre, C. O.; Lee, J.; Gabardi, R.; Choi, M. C.; Shin, K.; Parker, K. K. A bioinspired and hierarchically structured shape-memory material. *Nat. Mater.* **2021**, 20, 242–249
- (8) Fernandez-Gonzalez, R.; Zallen, J. A. Oscillatory behaviors and hierarchical assembly of contractile structures in intercalating cells. *Phys. Biol.* **2011**, *8*, 045005.
- (9) Kostiainen, M. A.; Kasyutich, O.; Cornelissen, J. J.; Nolte, R. J. Self-assembly and optically triggered disassembly of hierarchical dendron-virus complexes. *Nat. Chem.* **2010**, *2*, 394–399.
- (10) Skorupka, K. A.; Roganowicz, M. D.; Christensen, D. E.; Wan, Y.; Pornillos, O.; Ganser-Pornillos, B. K. Hierarchical assembly governs TRIM5 α recognition of HIV-1 and retroviral capsids. *Sci. Adv.* **2019**, 5, No. eaaw3631.
- (11) Fan, L.; Li, J.-L.; Cai, Z.; Wang, X. Bioactive hierarchical silk fibers created by bioinspired self-assembly. *Nat. Commun.* **2021**, *12*, 1–9.
- (12) Wang, Y.; Huang, X.; Zhang, X. Ultrarobust, tough and highly stretchable self-healing materials based on cartilage-inspired non-covalent assembly nanostructure. *Nat. Commun.* **2021**, *12*, 1–10.
- (13) Sang, Y.; Liu, M. Hierarchical self-assembly into chiral nanostructures. Chem. Sci. 2022, 13, 633-656.
- (14) Finnemore, A.; Cunha, P.; Shean, T.; Vignolini, S.; Guldin, S.; Oyen, M.; Steiner, U. Biomimetic layer-by-layer assembly of artificial nacre. *Nat. Commun.* **2012**, *3*, 1–6.
- (15) Olson, S. K.; Greenan, G.; Desai, A.; Müller-Reichert, T.; Oegema, K. Hierarchical assembly of the eggshell and permeability barrier in C. elegans. *J. Cell Biol.* **2012**, *198*, 731–748.
- (16) Do, D. T.; Singh, J.; Oey, I.; Singh, H. Biomimetic plant foods: Structural design and functionality. *Trends Food Sci. Technol.* **2018**, 82, 46–59.
- (17) Frederix, P. W.; Patmanidis, I.; Marrink, S. J. Molecular simulations of self-assembling bio-inspired supramolecular systems and their connection to experiments. *Chem. Soc. Rev.* **2018**, *47*, 3470–3489.

- (18) Prockop, D. J.; Fertala, A. The collagen fibril: the almost crystalline structure. *J. Struct. Biol.* **1998**, *122*, 111–118.
- (19) Furumaki, S.; Vacha, F.; Habuchi, S.; Tsukatani, Y.; Bryant, D. A.; Vacha, M. Absorption linear dichroism measured directly on a single light-harvesting system: the role of disorder in chlorosomes of green photosynthetic bacteria. *J. Am. Chem. Soc.* **2011**, *133*, 6703–6710.
- (20) Hoeben, F. J.; Jonkheijm, P.; Meijer, E.; Schenning, A. P. About supramolecular assemblies of π -conjugated systems. *Chem. Rev.* **2005**, 105, 1491–1546.
- (21) Orf, G. S.; Blankenship, R. E. Chlorosome antenna complexes from green photosynthetic bacteria. *Photosynth. Res.* **2013**, *116*, 315–331.
- (22) Scholes, G. D.; Fleming, G. R.; Olaya-Castro, A.; Van Grondelle, R. Lessons from nature about solar light harvesting. *Nat. Chem.* **2011**, *3*, 763–774.
- (23) Scholes, G. D.; Rumbles, G. Excitons in nanoscale systems. *Nat. Mater.* **2006**, *5*, 683–696.
- (24) Shibata, Y.; Saga, Y.; Tamiaki, H.; Itoh, S. Anisotropic distribution of emitting transition dipoles in chlorosome from Chlorobium tepidum: fluorescence polarization anisotropy study of single chlorosomes. *Photosynth. Res.* **2009**, *100*, 67–78.
- (25) Tian, Y.; Camacho, R.; Thomsson, D.; Reus, M.; Holzwarth, A. R.; Scheblykin, I. G. Organization of bacteriochlorophylls in individual chlorosomes from Chlorobaculum tepidum studied by 2-dimensional polarization fluorescence microscopy. *J. Am. Chem. Soc.* **2011**, *133*, 17192–17199.
- (26) Qi, R.; Jin, Y.; Cheng, X.; Fan, B.; Sun, T.; Peng, S.; Li, H. Crystallization-Driven Self-Assembly of Rod-Coil-Rod Pseudopolyrotaxanes into Spherical Micelles, Nanorods, and Nanorings in Aqueous Solutions. *Macromol. Rapid Commun.* **2015**, *36*, 1402–1408.
- (27) Terech, P.; Schaffhauser, V.; Maldivi, P.; Guenet, J. Living polymers in organic solvents. *Langmuir* **1992**, *8*, 2104–2106.
- (28) Asgari, M. A molecular model for the free energy, bending elasticity, and persistence length of wormlike micelles. *Eur. Phys. J. E* **2015**, 38, 1–16.
- (29) Patmanidis, I.; de Vries, A. H.; Wassenaar, T. A.; Wang, W.; Portale, G.; Marrink, S. J. Structural characterization of supramolecular hollow nanotubes with atomistic simulations and SAXS. *Phys. Chem. Chem. Phys.* **2020**, 22 (37), 21083–21093.
- (30) Kriete, B.; Lüttig, J.; Kunsel, T.; Malý, P.; Jansen, T. L.; Knoester, J.; Brixner, T.; Pshenichnikov, M. S. Interplay between structural hierarchy and exciton diffusion in artificial light harvesting. *Nat. Commun.* **2019**, *10*, 1–11.
- (31) Berlepsch, H. v.; Ludwig, K.; Böttcher, C. Pinacyanol chloride forms mesoscopic H-and J-aggregates in aqueous solution-a spectroscopic and cryo-transmission electron microscopy study. *Phys. Chem. Phys.* **2014**, *16*, 10659–10668.
- (32) Friedl, C.; Renger, T.; Berlepsch, H. v.; Ludwig, K.; Schmidt am Busch, M.; Megow, J. r. Structure prediction of self-assembled dye aggregates from cryogenic transmission electron microscopy, molecular mechanics, and theory of optical spectra. *Phys. Chem. C* **2016**, *120*, 19416–19433.
- (33) Milota, F.; Prokhorenko, V. I.; Mancal, T.; von Berlepsch, H.; Bixner, O.; Kauffmann, H. F.; Hauer, J. r. Vibronic and vibrational coherences in two-dimensional electronic spectra of supramolecular Jaggregates. *J. Phys. Chem. A* **2013**, *117*, 6007–6014.
- (34) Eisele, D. M.; Cone, C.; Bloemsma, E. A.; Vlaming, S.; Van Der Kwaak, C.; Silbey, R. J.; Bawendi, M. G.; Knoester, J.; Rabe, J. P.; Vanden Bout, D. Utilizing redox-chemistry to elucidate the nature of exciton transitions in supramolecular dye nanotubes. *Nat. Chem.* **2012**, *4*, 655–662.
- (35) Kumar, V.; Baker, G. A.; Pandey, S.; Baker, S. N.; Pandey, S. Contrasting behavior of classical salts versus ionic liquids toward aqueous phase J-aggregate dissociation of a cyanine dye. *Langmuir* **2011**, 27, 12884–12890.
- (36) Kriete, B.; Feenstra, C. J.; Pshenichnikov, M. S. Microfluidic out-of-equilibrium control of molecular nanotubes. *Phys. Chem. Chem. Phys.* **2020**, 22, 10179–10188.

- (37) Kirstein, S.; von Berlepsch, H.; Böttcher, C. Photo-induced reduction of Noble metal ions to metal nanoparticles on tubular Jaggregates. *Int. J. Photoenergy.* **2006**, 2006, 1–7.
- (38) Haverkort, F.; Stradomska, A.; de Vries, A. H.; Knoester, J. Investigating the structure of aggregates of an amphiphilic cyanine dye with molecular dynamics simulations. *J. Phys. Chem. B* **2013**, *117*, 5857–5867.
- (39) Von Berlepsch, H.; Regenbrecht, M.; Dähne, S.; Kirstein, S.; Böttcher, C. Surfactant-induced separation of stacked J-aggregates. Cryo-transmission electron microscopy studies reveal bilayer ribbons. *Langmuir* **2002**, *18*, 2901–2907.
- (40) Schade, B.; Singh, A. K.; Wycisk, V.; Cuellar-Camacho, J. L.; von Berlepsch, H.; Haag, R.; Böttcher, C. Stereochemistry-Controlled Supramolecular Architectures of New Tetrahydroxy-Functionalised Amphiphilic Carbocyanine Dyes. *Chem.—Eur. J.* **2020**, *26*, 6919–6934.
- (41) von Berlepsch, H.; Kirstein, S.; Hania, R.; Didraga, C. t. l.; Pugžlys, A.; Böttcher, C. Stabilization of individual tubular Jaggregates by poly (vinyl alcohol). *J. Phys. Chem. B* **2003**, *107*, 14176–14184.
- (42) von Berlepsch, H.; Kirstein, S.; Böttcher, C. Controlling the helicity of tubular J-aggregates by chiral alcohols. *J. Phys. Chem. B* **2003**, *107*, 9646–9654.
- (43) Von Berlepsch, H.; Kirstein, S.; Böttcher, C. Effect of alcohols on J-aggregation of a carbocyanine dye. *Langmuir* **2002**, *18*, 7699–7705.
- (44) Mattia, E.; Otto, S. Supramolecular systems chemistry. *Nat. Nanotechnol.* **2015**, *10*, 111–119.
- (45) Dong, S.; Zheng, B.; Xu, D.; Yan, X.; Zhang, M.; Huang, F. A crown ether appended super gelator with multiple stimulus responsiveness. *Adv. Mater.* **2012**, *24*, 3191–3195.
- (46) Li, S.-L.; Xiao, T.; Lin, C.; Wang, L. Advanced supramolecular polymers constructed by orthogonal self-assembly. *Chem. Soc. Rev.* **2012**, *41*, 5950–5968.
- (47) Li, S.-L.; Xiao, T.; Wu, Y.; Jiang, J.; Wang, L. New linear supramolecular polymers that are driven by the combination of quadruple hydrogen bonding and crown ether-paraquat recognition. *Chem. comm.* **2011**, *47*, 6903–6905.
- (48) Niu, Z.; Gibson, H. W. Polycatenanes. Chem. Rev. 2009, 109, 6024-6046.
- (49) Zhang, M.; Li, S.; Dong, S.; Chen, J.; Zheng, B.; Huang, F. Preparation of a daisy chain via threading-followed-by-polymerization. *Macromolecules* **2011**, *44*, 9629–9634.
- (50) Zhang, M.; Xu, D.; Yan, X.; Chen, J.; Dong, S.; Zheng, B.; Huang, F. Self-healing supramolecular gels formed by crown ether based host-guest interactions. *Angew. Chem., Int. Ed.* **2012**, *124*, 7117–7121.
- (51) Zhang, Z.; Luo, Y.; Chen, J.; Dong, S.; Yu, Y.; Ma, Z.; Huang, F. Formation of Linear Supramolecular Polymers That Is Driven by CH center dot center dot center dot pi Interactions in Solution and in the Solid State. *Angew. Chem., Int. Ed.* **2011**, *50*, 1397–1401.
- (52) Marsat, J.-N.; Heydenreich, M.; Kleinpeter, E.; Berlepsch, H. v.; Böttcher, C.; Laschewsky, A. Self-Assembly into Multicompartment Micelles and Selective Solubilization by Hydrophilic-Lipophilic-Fluorophilic Block Copolymers. *Macromolecules* **2011**, *44*, 2092–2105.
- (53) Yan, Y.; Huang, J.; Tang, B. Z. Kinetic trapping-a strategy for directing the self-assembly of unique functional nanostructures. *Chem. comm.* **2016**, *52*, 11870–11884.
- (54) Megow, J.; Rohr, M. I. S.; Schmidt am Busch, M.; Renger, T.; Mitric, R.; Kirstein, S.; Rabe, J. P.; May, V. Site-dependence of van der Waals interaction explains exciton spectra of double-walled tubular Jaggregates. *Phys. Chem. Chem. Phys.* **2015**, *17*, 6741–6747.
- (55) Clark, K. A.; Krueger, E. L.; Vanden Bout, D. A. Direct measurement of energy migration in supramolecular carbocyanine dye nanotubes. *J. Phys. Chem. Lett.* **2014**, *5*, 2274–2282.
- (56) Eisele, D. M.; Berlepsch, H. v.; Bottcher, C.; Stevenson, K. J.; Vanden Bout, D. A.; Kirstein, S.; Rabe, J. r. P. Photoinitiated growth

- of sub-7 nm silver nanowires within a chemically active organic nanotubular template. *J. Am. Chem. Soc.* **2010**, *132*, 2104–2105.
- (57) Bondarenko, A. S.; Jansen, T. L.; Knoester, J. Exciton localization in tubular molecular aggregates: Size effects and optical response. *J. Chem. Phys.* **2020**, *152*, 194302.
- (58) Bondarenko, A. S.; Patmanidis, I.; Alessandri, R.; Souza, P. C.; Jansen, T. L.; de Vries, A. H.; Marrink, S. J.; Knoester, J. Multiscale modeling of molecular structure and optical properties of complex supramolecular aggregates. *Chem. Sci.* **2020**, *11*, 11514–11524.
- (59) Haverkort, F.; Stradomska, A.; de Vries, A. H.; Knoester, J. First-principles calculation of the optical properties of an amphiphilic cyanine dye aggregate. *J. Phys. Chem. A* **2014**, *118*, 1012–1023.
- (60) Haverkort, F.; Stradomska, A.; Knoester, J. First-principles simulations of the initial phase of self-aggregation of a cyanine dye: Structure and optical spectra. *J. Phys. Chem. B* **2014**, *118*, 8877–8890.
- (61) Imura, K.; Mizobata, H.; Makita, Y. Photobleaching-Assisted Near-Field Absorption Spectroscopy: Its Application to Single Tubular J-Aggregates. *Bull. Chem. Soc. Jpn.* **2016**, *89*, 1518–1522.
- (62) Kriete, B. r.; Bondarenko, A. S.; Jumde, V. R.; Franken, L. E.; Minnaard, A. J.; Jansen, T. L.; Knoester, J.; Pshenichnikov, M. S. Steering self-assembly of amphiphilic molecular nanostructures via halogen exchange. *J. Phys. Chem. Lett.* **2017**, *8*, 2895–2901.
- (63) Kriete, B. r.; Bondarenko, A. S.; Alessandri, R.; Patmanidis, I.; Krasnikov, V. V.; Jansen, T. L.; Marrink, S. J.; Knoester, J.; Pshenichnikov, M. S. Molecular versus excitonic disorder in individual artificial light-harvesting systems. *J. Am. Chem. Soc.* **2020**, *142*, 18073–18085.
- (64) Krishnaswamy, S. R.; Gabrovski, I. A.; Patmanidis, I.; Stuart, M. C.; de Vries, A. H.; Pshenichnikov, M. S. Cryogenic TEM imaging of artificial light harvesting complexes outside equilibrium. *Sci. Rep.* **2022**, *12*, 1–8.
- (65) Didraga, C.; Pugžlys, A.; Hania, P. R.; von Berlepsch, H.; Duppen, K.; Knoester, J. Structure, spectroscopy, and microscopic model of tubular carbocyanine dye aggregates. *J. Phys. Chem. B* **2004**, 108, 14976–14985.
- (66) Pugžlys, A.; Augulis, R.; Van Loosdrecht, P.; Didraga, C.; Malyshev, V.; Knoester, J. Temperature-dependent relaxation of excitons in tubular molecular aggregates: fluorescence decay and Stokes shift. *J. Phys. Chem. B* **2006**, *110*, 20268–20276.
- (67) Berlepsch, H. v.; Ludwig, K.; Kirstein, S.; Böttcher, C. Mixtures of achiral amphiphilic cyanine dyes form helical tubular J-aggregates. *Chem. Phys.* **2011**, 385, 27–34.
- (68) von Berlepsch, H.; Kirstein, S.; Hania, R.; Pugžlys, A.; Böttcher, C. Modification of the nanoscale structure of the J-aggregate of a sulfonate-substituted amphiphilic carbocyanine dye through incorporation of surface-active additives. *J. Phys. Chem. B* **2007**, *111*, 1701–1711.
- (69) Eisele, D. M.; Arias, D. H.; Fu, X.; Bloemsma, E. A.; Steiner, C. P.; Jensen, R. A.; Rebentrost, P.; Eisele, H.; Tokmakoff, A.; Lloyd, S.; et al. Robust excitons inhabit soft supramolecular nanotubes. *Proc. Natl. Acad. Sci. U.S.A.* **2014**, *111*, E3367–E3375.
- (70) Plehn, T.; Ziemann, D.; Megow, J. r.; May, V. Frenkel to Wannier-Mott exciton transition: calculation of FRET rates for a tubular dye aggregate coupled to a CdSe nanocrystal. *J. Phys. Chem. B* **2015**, *119*, 7467–7472.
- (71) Didraga, C.; Klugkist, J. A.; Knoester, J. Optical properties of helical cylindrical molecular aggregates: the homogeneous limit. *J. Phys. Chem. B* **2002**, *106*, 11474–11486.
- (72) Von Berlepsch, H.; Böttcher, C.; Ouart, A.; Burger, C.; Dähne, S.; Kirstein, S. Supramolecular structures of J-aggregates of carbocyanine dyes in solution. *J. Phys. Chem. B* **2000**, *104*, 5255–5262.
- (73) Würthner, F.; Kaiser, T. E.; Saha-Möller, C. R. J-aggregates: from serendipitous discovery to supramolecular engineering of functional dye materials. *Angew. Chem., Int. Ed.* **2011**, *50*, 3376–3410.
- (74) Hestand, N. J.; Spano, F. C. Expanded theory of H-and J-molecular aggregates: the effects of vibronic coupling and intermolecular charge transfer. *Chem. Rev.* **2018**, *118*, 7069–7163.

- (75) Kasha, M.; Rawls, H. R.; Ashraf El-Bayoumi, M. The exciton model in molecular spectroscopy. *Pure Appl. Chem.* **1965**, *11*, 371–392.
- (76) Caram, J. R.; Doria, S.; Eisele, D. r. M.; Freyria, F. S.; Sinclair, T. S.; Rebentrost, P.; Lloyd, S.; Bawendi, M. G. Room-temperature micron-scale exciton migration in a stabilized emissive molecular aggregate. *Nano Lett.* **2016**, *16*, 6808–6815.
- (77) Freyria, F. S.; Cordero, J. M.; Caram, J. R.; Doria, S.; Dodin, A.; Chen, Y.; Willard, A. P.; Bawendi, M. G. Near-infrared quantum dot emission enhanced by stabilized self-assembled j-aggregate antennas. *Nano Lett.* **2017**, *17*, 7665–7674.
- (78) Kumar, V.; Baker, G. A.; Pandey, S. Ionic liquid-controlled Jversus H-aggregation of cyanine dyes. *Chem. comm.* **2011**, 47, 4730–4732
- (79) Patmanidis, I.; Souza, P. C.; Sami, S.; Havenith, R. W.; de Vries, A. H.; Marrink, S. J. Modelling structural properties of cyanine dye nanotubes at coarse-grained level. *Nanoscale Adv.* **2022**, *4*, 3033.
- (80) Bloemsma, E.; Vlaming, S.; Malyshev, V.; Knoester, J. Signature of Anomalous Exciton Localization in the Optical Response of Self-Assembled Organic Nanotubes. *Phys. Rev. Lett.* **2015**, *114*, 156804.
- (81) Vlaming, S. M.; Bloemsma, E. A.; Nietiadi, M. L.; Knoester, J. Disorder-induced exciton localization and violation of optical selection rules in supramolecular nanotubes. *J. Chem. Phys.* **2011**, 134, 114507.
- (82) Didraga, C.; Knoester, J. Optical spectra and localization of excitons in inhomogeneous helical cylindrical aggregates. *J. Chem. Phys.* **2004**, *121*, 10687–10698.
- (83) Qiao, Y.; Polzer, F.; Kirmse, H.; Steeg, E.; Kühn, S.; Friede, S.; Kirstein, S.; Rabe, J. r. P. Nanotubular J-aggregates and quantum dots coupled for efficient resonance excitation energy transfer. *ACS Nano* **2015**, *9*, 1552–1560.
- (84) Zhang, Y.; Lou, H.; Zhang, W.; Wang, M. Mussel-Inspired Surface Coating to Stabilize and Functionalize Supramolecular J-Aggregate Nanotubes Composed of Amphiphilic Cyanine Dyes. *Langmuir* **2022**, *38*, 8160–8168.
- (85) Dai, H.; Huang, W.; Zeng, Q. Temperature-induced self-assembly transformation: an effective external stimulus on 2D supramolecular structures. *New J. Chem.* **2022**, *46*, 9965.
- (86) Gutzler, R.; Sirtl, T.; Dienstmaier, J. r. F.; Mahata, K.; Heckl, W. M.; Schmittel, M.; Lackinger, M. Reversible phase transitions in self-assembled monolayers at the liquid-solid interface: temperature-controlled opening and closing of nanopores. *J. Am. Chem. Soc.* **2010**, 132, 5084–5090.
- (87) Klein, M. D.; Shulenberger, K. E.; Barotov, U.; Šverko, T.; Bawendi, M. G. Supramolecular Lattice Deformation and Exciton Trapping in Nanotubular J-Aggregates. *J. Phys. Chem. C* **2022**, *126*, 4095–4105.
- (88) Doria, S.; Di Donato, M.; Borrelli, R.; Gelin, M. F.; Caram, J.; Pagliai, M.; Foggi, P.; Lapini, A. Vibronic coherences in light harvesting nanotubes: unravelling the role of dark states. *J. Mater. Chem. C* **2022**, *10*, 7216–7226.
- (89) Spitz, C.; Knoester, J.; Ouart, A.; Daehne, S. Polarized absorption and anomalous temperature dependence of fluorescence depolarization in cylindrical J-aggregates. *Chem. Phys.* **2002**, *275*, 271–284.
- (90) Lampoura, S.; Spitz, C.; Dähne, S.; Knoester, J.; Duppen, K. The optical dynamics of excitons in cylindrical J-aggregates. *J. Phys. Chem. B* **2002**, *106*, 3103–3111.
- (91) Clark, K. A.; Krueger, E. L.; Vanden Bout, D. A. Temperature-dependent exciton properties of two cylindrical J-aggregates. *J. Phys. Chem. C* **2014**, *118*, 24325–24334.
- (92) Watanabe, T.; Shiga, M.; Asai, K.; Ishigure, K. The influence of counter ions on the morphology of cyanine dye aggregates at the air/water interface. *Molecular Crystals and Liquid Crystals Science and Technology. Section A. Mol. Cryst. Liq. Cryst.* 1999, 327, 135–138.
- (93) Clark, K. A.; Cone, C. W.; Vanden Bout, D. A. Quantifying the polarization of exciton transitions in double-walled nanotubular Jaggregates. J. Phys. Chem. C 2013, 117, 26473–26481.

- (94) Male, K. B.; Li, J.; Bun, C. C.; Ng, S.-C.; Luong, J. H. Synthesis and stability of fluorescent gold nanoparticles by sodium borohydride in the presence of mono-6-deoxy-6-pyridinium- β -cyclodextrin chloride. *J. Phys. Chem. C* **2008**, *112*, 443–451.
- (95) Wagner, J.; Tshikhudo, T.; Köhler, J. Microfluidic generation of metal nanoparticles by borohydride reduction. *J. Chem. Eng.* **2008**, 135, S104–S109.
- (96) Polte, J.; Erler, R.; Thunemann, A. F.; Sokolov, S.; Ahner, T. T.; Rademann, K.; Emmerling, F.; Kraehnert, R. Nucleation and growth of gold nanoparticles studied via in situ small angle X-ray scattering at millisecond time resolution. *ACS Nano* **2010**, *4*, 1076–1082.
- (97) Struganova, I. A.; Hazell, M.; Gaitor, J.; McNally-Carr, D.; Zivanovic, S. Influence of Inorganic Salts and Bases on the J-Band in the Absorption Spectra of Water Solutions of 1,1'-Diethyl-2,2'-cyanine Iodide. *J. Phys. Chem. A* **2003**, *107*, 2650–2656.
- (98) Struganova, I. A.; Lim, H.; Morgan, S. A. The Influence of Inorganic Salts and Bases on the Formation of the J-band in the Absorption and Fluorescence Spectra of the Diluted Aqueous Solutions of TDBC. J. Phys. Chem. B 2002, 106, 11047–11050.
- (99) Thomas, S. P.; Dikundwar, A. G.; Sarkar, S.; Pavan, M. S.; Pal, R.; Hathwar, V. R.; Row, T. N. G. The Relevance of Experimental Charge Density Analysis in Unraveling Noncovalent Interactions in Molecular Crystals. *Molecules* **2022**, *27*, 3690.
- (100) Popa, I.; Gillies, G.; Papastavrou, G.; Borkovec, M. Attractive and Repulsive Electrostatic Forces between Positively Charged Latex Particles in the Presence of Anionic Linear Polyelectrolytes. *J. Phys. Chem. B* **2010**, *114*, 3170–3177.
- (101) von Berlepsch, H.; Kirstein, S.; Böttcher, C. Supramolecular structure of J-aggregates of a sulfonate substituted amphiphilic carbocyanine dye in solution: Methanol-induced ribbon-to-tubule transformation. *J. Phys. Chem. B* **2004**, *108*, 18725–18733.
- (102) Lyon, J. L.; Eisele, D. M.; Kirstein, S.; Rabe, J. P.; Vanden Bout, D. A.; Stevenson, K. J. Spectroelectrochemical investigation of double-walled tubular J-aggregates of amphiphilic cyanine dyes. *J. Phys. Chem. C* **2008**, *112*, 1260–1268.
- (103) Weber, C. M.; Eisele, D. M.; Rabe, J. P.; Liang, Y.; Feng, X.; Zhi, L.; Müllen, K.; Lyon, J. L.; Williams, R.; Bout, D. A. V.; et al. Graphene-based optically transparent electrodes for spectroelectrochemistry in the UV-Vis region. *Small* **2010**, *6*, 184–189.
- (104) Steeg, E.; Polzer, F.; Kirmse, H.; Qiao, Y.; Rabe, J. P.; Kirstein, S. Nucleation, growth, and dissolution of silver nanostructures formed in nanotubular J-aggregates of amphiphilic cyanine dyes. *J. Colloid Interface Sci.* **2016**, 472, 187–194.
- (105) Shrestha, S.; Wang, B.; Dutta, P. Nanoparticle processing: Understanding and controlling aggregation. *Adv. Colloid Interface Sci.* **2020**, 279, 102162.
- (106) Kometani, N.; Nakajima, H.; Asami, K.; Yonezawa, Y.; Kajimoto, O. Excited-state dynamics of the mixed J-aggregate of two kinds of cyanine dyes in layer-by-layer alternate assemblies. *Chem. Phys. Lett.* **1998**, 294, 619–624.
- (107) Yoshida, A.; Yonezawa, Y.; Kometani, N. Tuning of the Spectroscopic Properties of Composite Nanoparticles by the Insertion of a Spacer Layer: Effect of Exciton- Plasmon Coupling. *Langmuir* **2009**, *25*, 6683–6689.
- (108) Fofang, N. T.; Grady, N. K.; Fan, Z.; Govorov, A. O.; Halas, N. J. Plexciton Dynamics: Exciton Plasmon Coupling in a J-Aggregate Au Nanoshell Complex Provides a Mechanism for Nonlinearity. *Nano Lett.* **2011**, *11*, 1556–1560.
- (109) Qiao, Y.; Polzer, F.; Kirmse, H.; Steeg, E.; Kirstein, S.; Rabe, J. P. In situ synthesis of semiconductor nanocrystals at the surface of tubular J-aggregates. *J. Mater. Chem. C* **2014**, *2*, 9141–9148.
- (110) Al-Khatib, O.; Böttcher, C.; von Berlepsch, H.; Herman, K.; Schön, S.; Rabe, J. P.; Kirstein, S. Adsorption of polyelectrolytes onto the oppositely charged surface of tubular J-aggregates of a cyanine dye. *Colloid Polym. Sci.* **2019**, 297, 729–739.
- (111) Von Berlepsch, H.; De Vries, R. Weakly charged lamellar bilayer system: Interplay between thermal undulations and electrostatic repulsion. *Eur. Phys. J. E* **2000**, *1*, 141–152.

- (112) Ng, K.; Webster, M.; Carbery, W. P.; Visaveliya, N.; Gaikwad, P.; Jang, S. J.; Kretzschmar, I.; Eisele, D. M. Frenkel excitons in heat-stressed supramolecular nanocomposites enabled by tunable cage-like scaffolding. *Nat. Chem.* **2020**, *12*, 1157–1164.
- (113) Eisele, D. M.; Knoester, J.; Kirstein, S.; Rabe, J. P.; Vanden Bout, D. A. Uniform exciton fluorescence from individual molecular nanotubes immobilized on solid substrates. *Nat. Nanotechnol.* **2009**, *4*, 658–663.